ISSN 0915-633X

NATIONAL INSTITUTE FOR FUSION SCIENCE

Electric Field Profile of CHS Heliotron Torsatron Plasma with Tangential Neutral Beam Injection

K. Ida, H. Yamada, H. Iguchi, S. Hidekuma, H. Sanuki,
K. Yamazaki and CHS Group

(Received – Sep. 20, 1990)

NIFS-60 Oct. 1990

RESEARCH REPORT
NIFS Series

NAGOYA, JAPAN

Electric field profile of CHS Heliotron/Torsatron plasma with tangential neutral beam injection

K.Ida, H.Yamada, H.Iguchi, S.Hidekuma,
H.Sanuki, K.Yamazaki and CHS Group

National Institute for Fusion Science,
Nagoya, 464-01, JAPAN

Abstract

The radial electric field profiles derived from poloidal rotation velocity are compared with neoclassical estimates for a plateau regime plasma heated by tangentially injected neutral beam in CHS heliotron/torsatron device. The measured electric field (E_r) is more negative than the neoclassical prediction especially near the plasma periphery. A gradient of radial electric field ($\partial E_r/\partial r$) in this region is found to be more negative in the plasma with higher electron density. Although the corresponding poloidal rotation velocity is too small to trigger the L/H transition, these negative E_r and $\partial E_r/\partial r$ are associated with a reduction of thermal electron conductivity.

"keyword" radial electric field, poloidal rotation, CHS Heliotron/Torsatron, tangential neutral beam injection

Recently a radial electric field (E_r) near the plasma periphery has been found to play an important role in plasma confinement especially in H-mode[1,2]. The negative electric field or negative gradient ($\partial E_r/\partial r$) is expected to reduce the electron anomalous loss by suppressing micro-instability[3,4]. In a Heliotron/Torsatron device, the neoclassical theory predicts that an electric field also reduces helical ripple loss and improve the energy confinement[5,6]. Thus it is crucial to measure the electric field (and its gradient) and to compare neoclassical estimates and a reduction of electron thermal conductivity.

The poloidal rotation only near the plasma periphery has been measured with intrinsic impurity radiation in the Wendelstein VII-A Stellarator and Heliotron-E devices[7,8]. In these devices, neutral beams are injected almost perpendicular to magnetic field and the significant loss cone of ions exist in the plasma. Large negative electric field has been explained to be built up by the fast ion loss of perpendicular neutral beam injection (NBI) in the Wendelstein VII-A[7]. However, in the Compact Helical System (CHS)[9], a neutral beam is injected tangentially and there is no loss cone for the injected fast ions. The fast ion loss does not play an important role any more and the electric filed is determined by the balance of bulk electron and ion fluxes. In this paper, we present the measurements of electric field profiles derived from both toroidal and poloidal rotation velocities and pressure gradients in the whole plasma by using charge exchange spectroscopy(CXS).

The Compact Helical System (CHS), is the poloidal period number $l = 2$ and toroidal period number $m = 8$ heliotron/torsatron device with a major radius of 100 cm and an average minor radius of 20 cm. The aspect ratio $1/\varepsilon$ is 5, which is comparable to those in tokamaks. However, a safety factor of q ($=\varepsilon B/B_\theta$) of the magnetic field is much smaller (~ 1) than those in tokamaks (typically 2.5 ~ 5). A

28 GHz gyrotron with an injection power of 100 kW produces ECH plasma with a low density below 1 x 10^{13} cm^{-3} , while the tangential NBI with 0.9 MW can sustain the plasma with high density up to 1 x 10^{14} cm^{-3}. A 128 channel space resolved 1 m visible spectrometer system using a CCD detector coupled with an image intensifier has been developed to measure the ion temperature and poloidal/toroidal rotation velocities[10].

Four sets of optical fiber array have been installed in CHS. Two of them (one poloidally and the other toroidally) are viewing a fast neutral beam poloidally and the other two are viewing not intersecting the neutral beam line to subtract background radiation. These optical fibers with 100 μ mm diameter are led into the entrance slit of 1 m Czerny-Turner spectrometer with 2400 grooves/mm grating. At the exit plane, the light from each fiber gives the spectrum from one spatial position. The light from all of the fibers is focused onto the image intensifier tube coupled with a CCD TV camera. The resolution is 0.1 Å/ch (100 spectral channels), while the time resolution is 16.7 ms. The background radiation is mostly due to the reaction between fully ionized impurities and background thermal neutrals in the plasma periphery. This background radiation emitted from the cool plasma edge is proportional to the neutral density at the plasma edge and depends on the clearance between plasma edge and inner wall (the position of magnetic axis) and or the amount of gas puff. Most measurements have been done using CVI 5292 Å (n = 8-7).

For ECH plasmas, the beam emission spectroscopy techniques can not be used due to the lack of a neutral beam. The intrinsic line radiation emitted from the plasma edge is measured to derive a poloidal rotation velocity. Even though the measurements of poloidal rotation cover the whole plasma region (84 cm < R < 107 cm), the measured velocities represent a chord average and the emission is localized at r=0.7a. The plasma rotates in the ion diamagnet direction with a velocity of 3 km/s for the low density (n_e = 4 x 10^{12} cm^{-3}) discharge produced by ECH.

The radial electric field averaged along the magnetic surface is 16 V/cm (positive). The central electron temperature is 900 eV. This indicates that the plasma potential is positive in the collisionless regime of ν_{*e} = 0.2, where ν_{*e} is electron collisionality normalized by plateau value. On the other hand, for an NBI plasma the beam emission spectroscopy technique is applicable. The emission is localized at the cross section between the neutral beam line (midplane) and the line of sight. The direction of measured rotation velocity is more likely poloidal at each point, although the space resolution becomes poor near the plasma center due to the integration effect along the neutral beam line. The plasma heated by NBI rotates in the electron diamag direction and has a strong shear near the plasma periphery. The poloidal rotation velocity at the plasma edge depends on the collisionality of the plasma.

Radial electric field profiles are obtained from the profiles of the ion pressure gradient $\partial p_I/\partial r$ and the toroidal/poloidal rotation (v_φ/v_θ) with the use of momentum balance equation,

$$E_r = \frac{\partial p_I}{eZ_I n_I \partial r} - (B_\theta V_\varphi - B_\varphi V_\theta),$$

where I stands for the measured impurity species. Here the radial frictional force between the different species is small enough to be neglected. The toroidal rotation velocity at r > 0.3a is damped to almost zero by the parallel viscosity caused by the helical ripple and has a very narrow profile at the center.

To investigate the dependence of collisionality, typical two discharges, one with low electron density (n_e = 1.5 x $10^{13}/cm^3$) and the other with high density (n_e = 6.0 x $10^{13}/cm^3$), are compared. The electron temperature and density profiles are measured with Thomson scattering as shown in Fig.1. The electron collisionality ν_{*e} at the half radius is 4.9 and 33 for the low density and high density cases, respectively. The ion temperature and poloidal rotation velocity profiles are measured with CXS as shown in Fig.2. The ion collisionality of ν_{*i} at the half radius is 3.6 for the low density discharge and 33 for the high density discharge. The ion temperature profile shows the significant Shafranov shift of magnetic axis due to the bulk and beam pressure. The Shafranov shift estimated by using finite β equilibrium code VMEC is 3 cm for high density case and 4.5 cm for the low density case[11]. The large shift in the low density case, which is also measured in the shift of ion temperature peak, is mainly due to the peaked parallel beam pressure driven by the tangential neutral beam. On the other hand, the magnetic axis shift in the high density case is due to thermal pressure.

The poloidal rotation profile for these discharges has a strong shear near the plasma edge. The poloidal rotation velocity shear results from the shear of radial electric field at the plasma periphery. Although the profile of poloidal rotation is similar to those observed in tokamak H-mode plasma[2], the poloidal rotation velocity is not large enough to trigger L/H transition. The poloidal rotation parameter $U_{p,m}$ $[=(v_\theta B)/(v_{th}B_\theta)+\lambda_p/2,\ \lambda_p=\rho_p(\partial p_i/\partial r)/p_i]$ is 0.2 for the low density case and 0.5 for the high density case. These values are much smaller than those observed in tokamak H-mode plasma (~ 4 in H-mode). This edge electric field estimated from momentum balance equation increases as the electron density is increased. This negative electric field is -80 V/cm for the low density and -120 V/cm for the high density plasma as shown in Fig.3. The radial electric field profiles measured in CHS are compared with the results based on the neoclassical theory presented by Kovrizhnykh[5] and Hastings[6]. These calculated electric field profiles are smaller than those measured from poloidal rotations. The electric field calculated with the Kovrizhnykh formula gives smaller values than that with the Hastings formula with multi-helicity effects. In the Kovrizhnykh formula, symmetric ambipolar fluxes play a role in reducing the electric field produced by the asymmetric ambipolar flux. However, these theories do not explain the electric field shear near the plasma edge. Ion orbit loss is a candidate to explain the large electric field measured near the plasma edge.

The radial electric field has been found to be related with the confinement improvement as observed in H-mode in tokamaks. An electron thermal diffusivity is evaluated with the analysis using ORNL PROCTR-mod code and the finite β equilibrium code VMEC for these plasmas. The electron thermal diffusivity is the lowest at $\rho = 0.7 \sim 0.9$, where the negative electric field and negative $\partial E_r/\partial r$ is observed. We note that both more negative electric filed and smaller electron thermal diffusivity are observed in the higher density case. More negative electric field should be enhanced, if only the electron flux (not ion flux) is reduced by the confinement improvement. Moreover, more negative electric filed is expected to suppress the electron anomalous loss. It is not clear that more negative electric field is a cause or result of reduction of electron thermal conductivity, because the analysis is in steady state. However, as in H-mode, the more negative electric filed is observed associated with the improvement of electron confinement. The difference with H-mode in tokamaks is that the reduction of thermal conductivity in CHS is not a bifurcation phenomena. Theoretically, the poloidal rotation parameter required for L/H transition in CHS is larger than those in tokamak, because of larger ripple of magnetic field. Even for the same values of poloidal rotation parameter, larger poloidal rotation velocity is required in CHS than in tokamak with similar aspect ratio because of low q value at the plasma periphery. However, the poloidal rotation velocity measured in CHS even for the high density case, is less than those measured in H-mode plasma in tokamaks, and is too small to trigger the bifurcation. Without any bifurcation of the poloidal rotation velocity, the reduction of thermal diffusivity is observed associated with negative electric field and negative gradient of electric field.

We would like to thank Drs. K.C.Shaing (ORNL), K.Itoh, S.-I.Itoh and Y.Ogawa for their useful discussions. Also thanks is due to S.Okamura, O.Kaneko, Y.Takeiri for their support of machine and NBI operation. We also thank the support of data acquisition by C.Takahashi and M.Kojima. Continuous encouragement by K.Matsuoka and support of CHS group are acknowledged.

References

[1]R.J.Groebner, K.H.Burrell, and R.P.Seraydarian Phys. Rev. Lett. **64** 3015 (1990).

[2]K.Ida et al., Phys. Rev. Lett. **65** 1364 (1990).

[3]S.-I.Itoh and K.Itoh, Phys. Rev. Lett. **60** 2276 (1988).

4K.C.Shaing and E.C.Crume Jr, Phys. Rev. Lett. **63** 2369 (1989).

[5]L.M.Kovrizhnykh, Nucl. Fusion **24** 435 (1984).

[6]D.E.Hastings, W.A.Houlberg, K.C.Shaing, Nucl. Fusion **25** 445 (1985).

[7]H.Wobig, et al., in Plasma Physics and Controlled Nuclear Fusion Research (in Proc. 11th IAEA Conf. Kyoto, 1986) Vol.II 369 (1986).

[8]K.Kondo, H. Zushi, S. Nishimura, et. al., Rev. Sci. Instrum. **59** 1533 (1988).

[9]K.Matsuoka et. al., in Plasma Physics and Controlled Nuclear Fusion Research (in Proc. 12th IAEA Conf. Nice, 1988) Vol.II 411 (1989).

[10]K.Ida and S. Hidekuma, Rev. Sci. Instrum. **60** 876 (1989).

[11]H.Yamada et al., in Proc. 1st Toki Conf., Toki, (1989).

Figure captions

Fig.1 Profiles of (a) electron density (n_e) and (b) temperature (T_e) measured with Thomson scattering for the plasma with the low density and the high density, where ν_{*e} is the normalized electron collisionality evaluated at the half of the plasma minor radius.

Fig.2 Profiles of (a) ion temperature (T_i) and (b) poloidal rotation velocity (v_θ) measured with charge exchange spectroscopy for the two cases in Fig.1, where ν_{*i} is the normalized ion collisionality evaluated at the half of the plasma minor radius. Arrows in Fig.(b) show the location of magnetic axis for vacuum magnetic field and finite β equilibrium.

Fig.3 Radial electric field profiles measured in CHS and neoclassical estimates. Solid lines are calculated radial electric field for the high density plasma, while the dashed lines for the low density plasma.

Fig.4 Radial profile of electron thermal diffusivity analyzed with ORNL PROCTR-mod code for the low and the high density plasma.

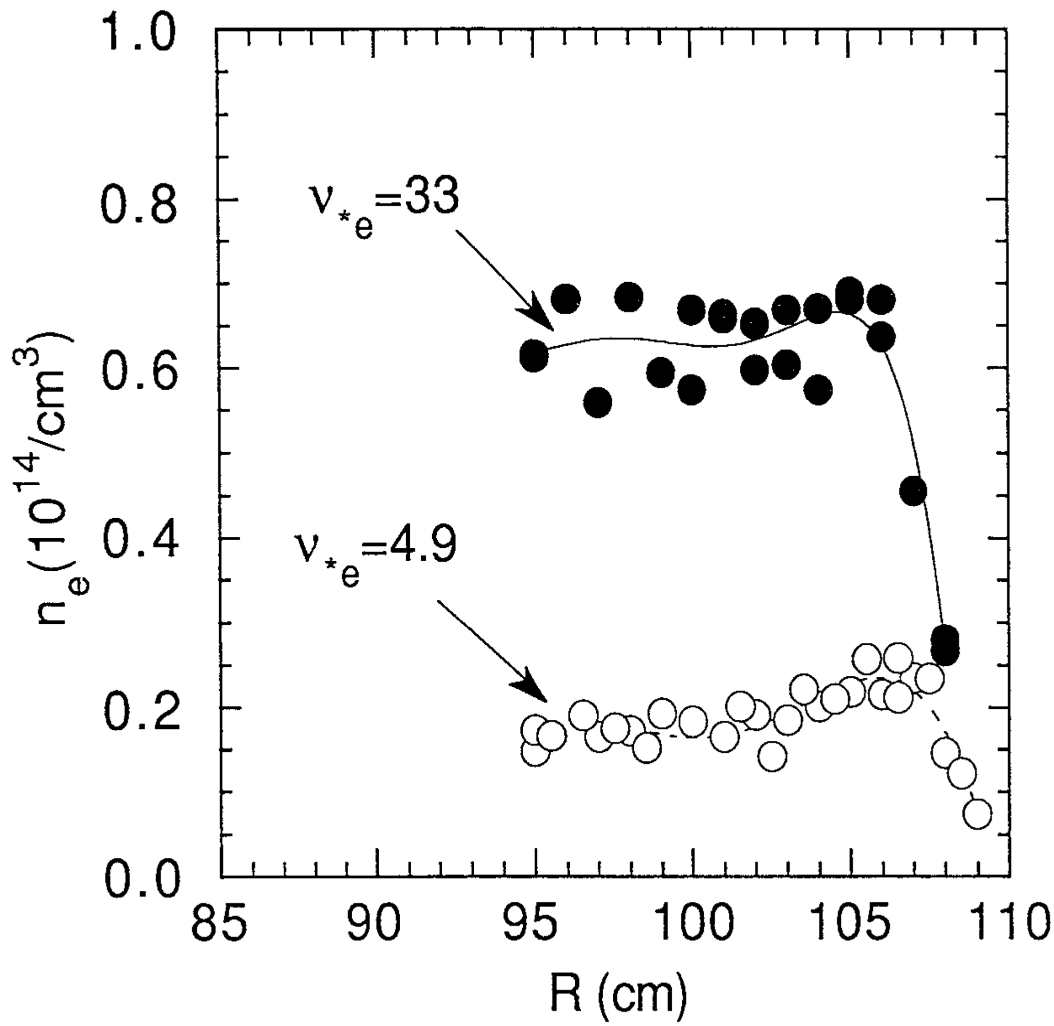

Figure 1 (a)

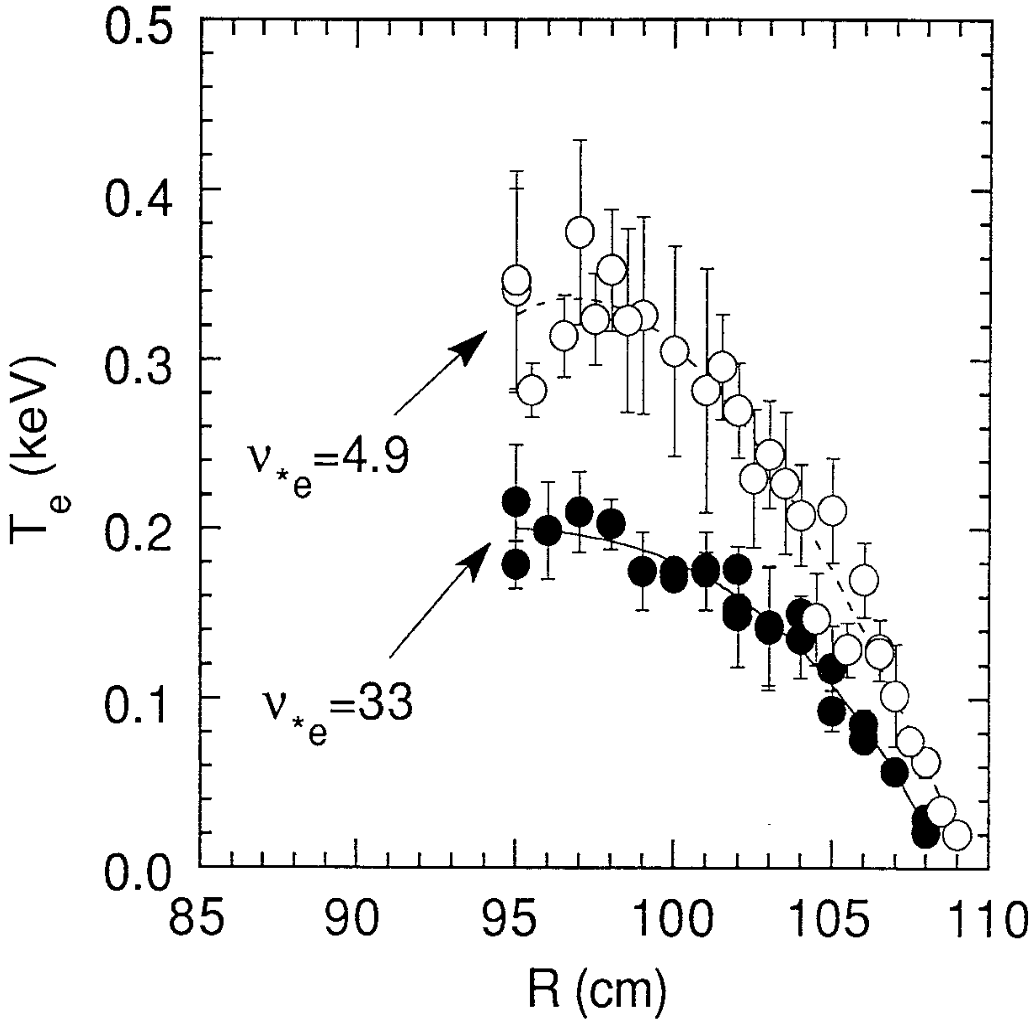

Figure 1 (b)

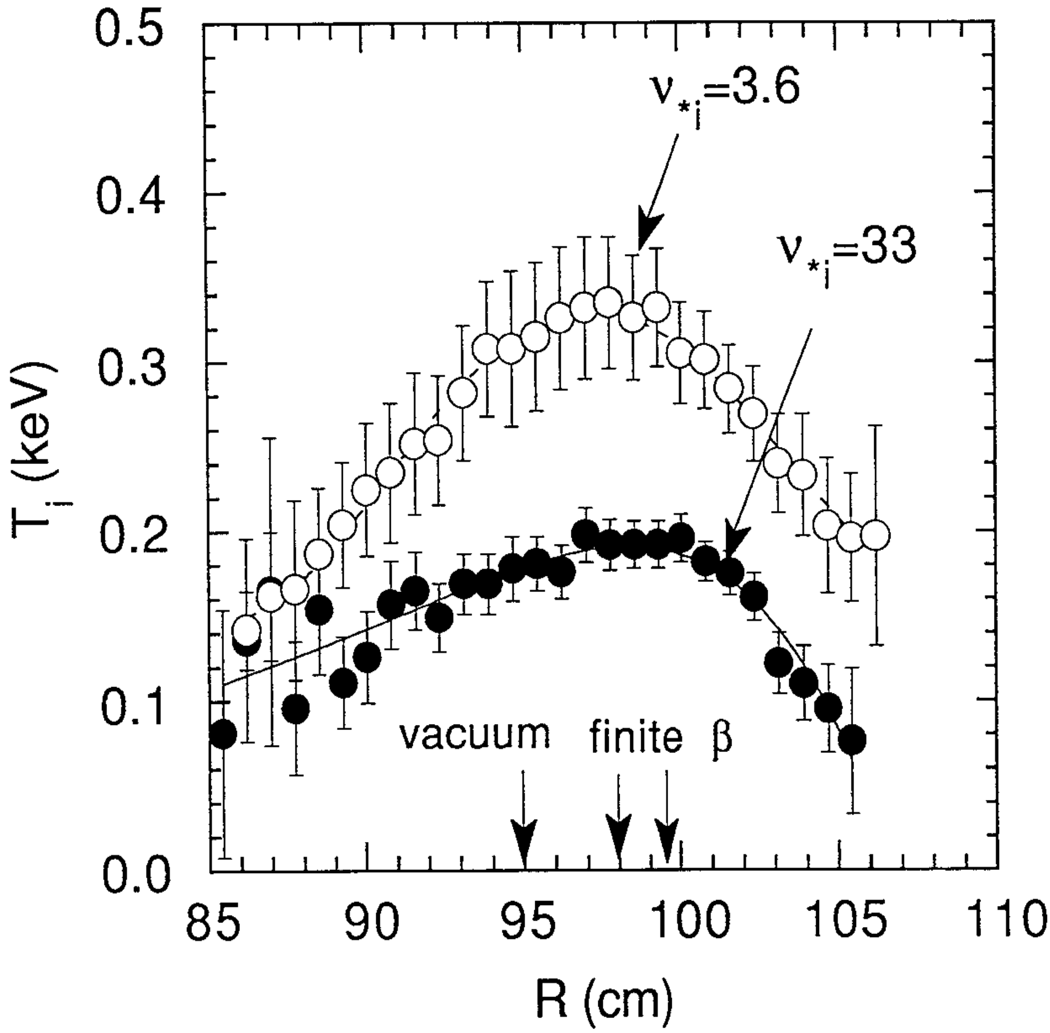

ν_{*i}=3.6
ν_{*i}=33
T_i (keV)
0.5
0.4
0.3
0.2
0.1
0.0
vacuum
finite β
85
90
95
100
105
110
R (cm)

Figure 2 (a)

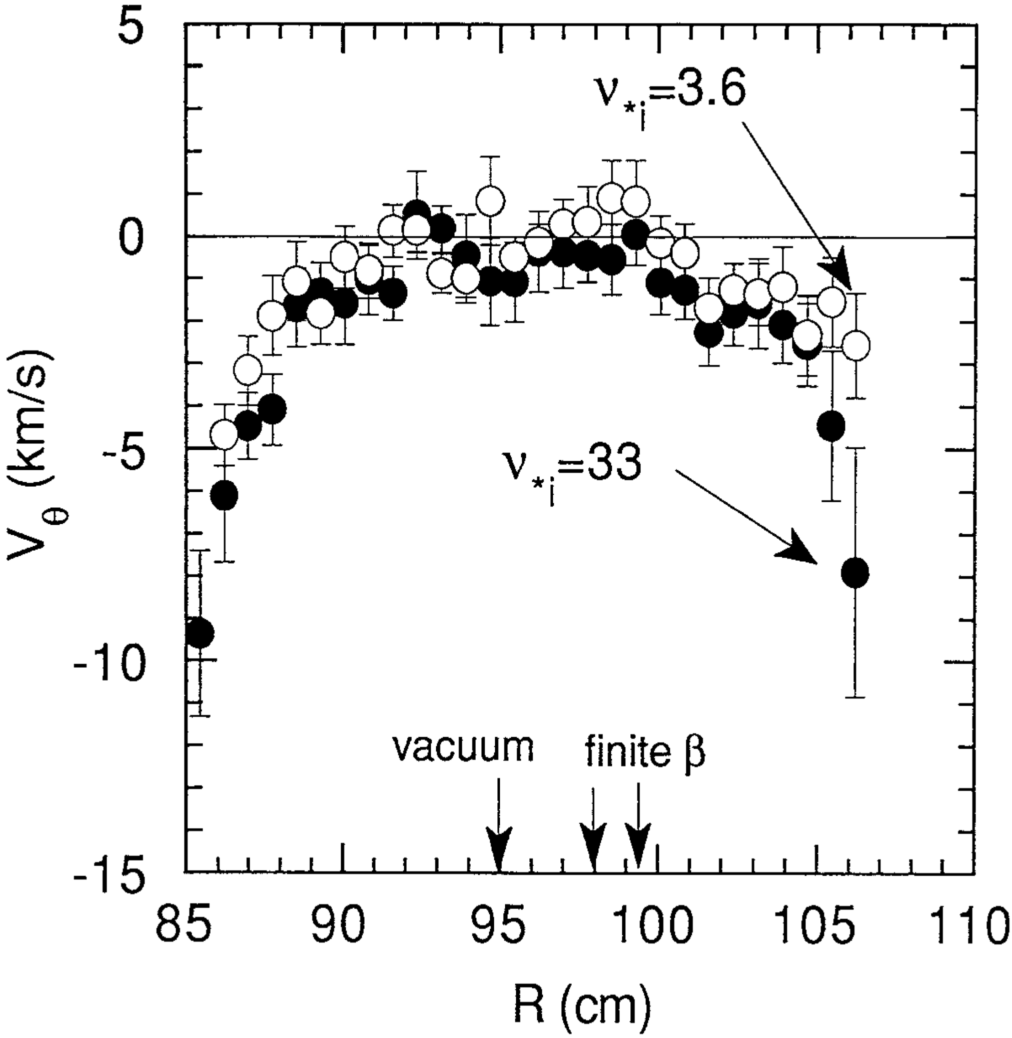

5
0
-5
-10
-15
85
90
95
100
105
110
V_θ (km/s)
R (cm)
ν_*i=3.6
ν_*i=33
vacuum
finite β

Figure 2 (b)

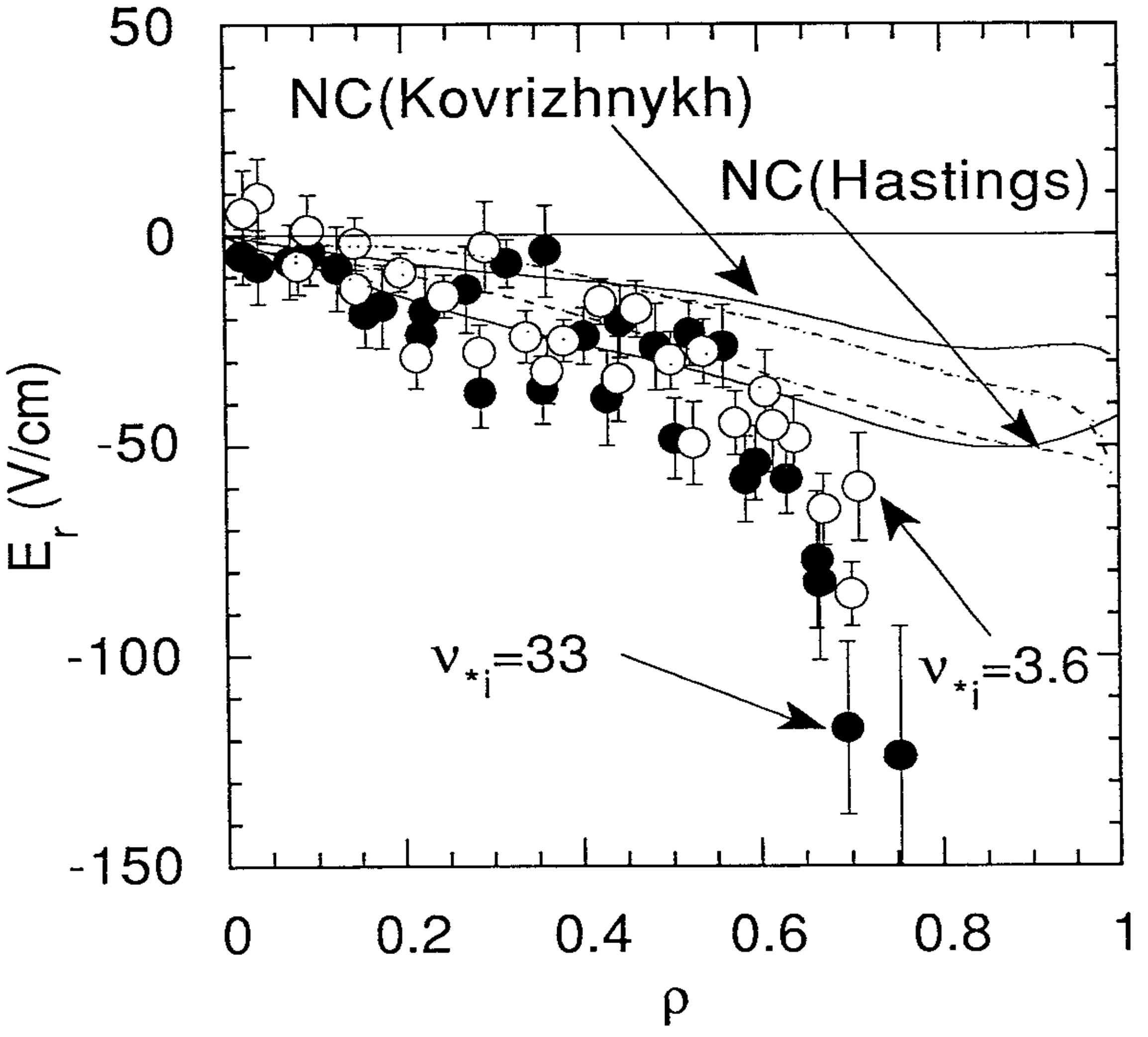
50
0
-50
-100
-150
0
0.2
0.4
0.6
0.8
1
E_r (V/cm)
ρ
NC(Kovrizhnykh)
NC(Hastings)
ν_{*i}=33
ν_{*i}=3.6

Figure 3

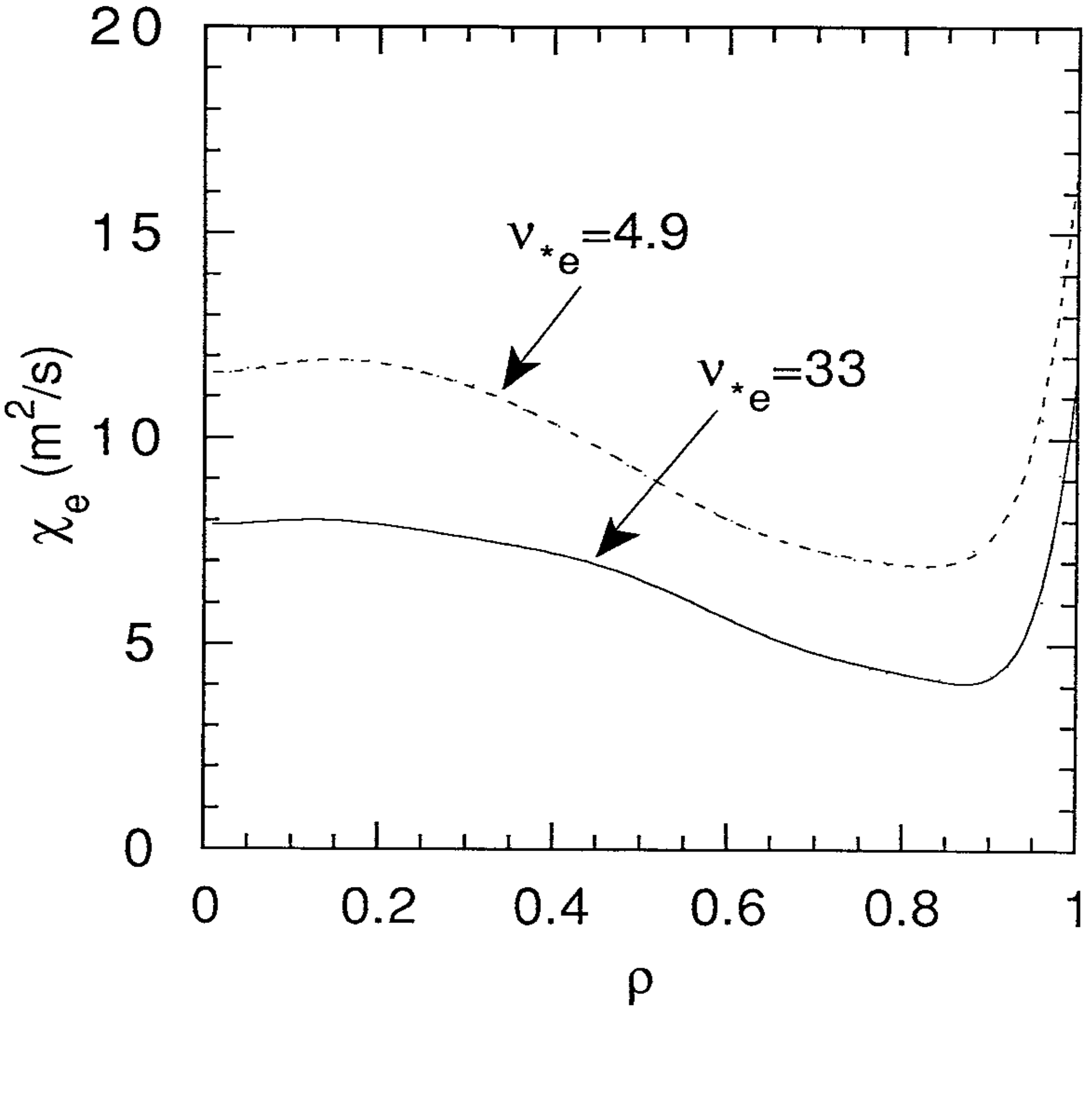

Figure 4